Investigating the Changes in Flux Density of Methanol Masers in the Orion Nebula

Maneth Perera
Illinois Mathematics and Science Academy
Advisor: Dr. E. D. Araya *(Western Illinois University)*
Collaborators: Gabriel Sojka, Kenneth VanZuiden *(Western Illinois University)*

Abstract

The VLA Orion-A Large Survey (VOLS) collaboration used the Karl G. Jansky Very Large Array (VLA) telescope to observe a methanol maser in the Orion Nebula 20 times from April 3rd, 2022 to July 1st, 2022, corresponding to 20 different epochs of data. This study aimed to characterize this methanol maser in terms of flux density consistency, fast variability, and light wave polarization on both a short-term and long-term scale using these data. We covered three main objectives: comparing pointing averages to see if flux density is consistent, checking for fast variability by plotting scan flux densities, and checking for linear or circular polarization. For objective 1, the flux density was consistent for 17 epochs and inconsistent for 3 epochs based on the measurement errors, insinuating consistent calibration between pointings for most epochs. For objective 2, within an epoch, some scans had clear trends but many had only slight differences in scan values, so we have no conclusive evidence of fast variability. For objective 3, we saw no linear or circular polarization in any of the epochs. We also saw many discrepancies in specific epochs such as offset pointing averages in epoch 2, an offset scan in epoch 3, negative sidelobes in a few epochs (mostly in epoch 10), and an error due to the software used to generate the images in epoch 11. While some of these discrepancies are explained by a lack of data or unusual signal calibrations, many are unexplained, which can suggest source variability. Through the study of many epochs in 2022, the maser's behavior on a short time scale was analyzed with

more accuracy than previous studies looking at averages over entire epochs.

Introduction

The Karl G. Jansky Very Large Array (VLA) is a radio telescope made of 27 separate antennae in New Mexico, U.S. It allows for data gathering in multiple different configurations of antennae, but for this project we used data from its B-configuration (arranging the telescopes in a Y-shape). The VOLS (VLA Orion-A Large Survey) is a collaborative effort by multiple researchers around the world, led by Dr. G. Busquet from the University of Barcelona, Spain, in order to map the Orion-A region, which includes the Orion Nebula (e.g., Sojka et al., 2024). These telescopes can point at different sections of the night sky, called pointings, to find stellar objects. If a stellar object appears in the overlap between these sections, we can use the separate measurements to confirm its position and signal strength. For this study, we took data from the VLA in 2022 on the dates April 3rd, 10th, 13th, 15th, 19th, 21st, 23rd, 24th; May 1st (2 epochs), 2nd, 3rd, 22nd, 24th; June 3rd, 4th, 7th, 10th, 14th; and July 1st labeled epochs 1 through 20, respectively. A previous study looked at the maser's average flux density over four of the epochs (Sojka et al., 2024). This work aimed to extend the analysis to more epochs and look at variability within specific epochs in order to further map out the maser's behavior over time.

The Orion Nebula is the closest high mass star forming region to Earth and therefore holds many accessible secrets about how star formation works, particularly high-mass star formation, i.e., stars with masses above 8 times the mass of the Sun. As a high-mass star forms, it goes through multiple phases, one of which includes a heated dense core releasing large

molecular outflow from two opposite poles (Motte et al., 2018). The energy released by the gravitational collapse of the core heats up the molecular gas so that the ejected molecules would be at excited states. Around the young stellar object, multiple clouds of high pressure gas can generate maser radiation, from excited spinning molecules (e.g., Motte et al., 2018). When stray photons in space, possibly from other nearby stellar objects, hit these molecules, the molecules emit a twin photon before spinning slower. Through this process, these clouds of gas emit microwave radiation in the form of these twin photons, which travel through space and can reach Earth after thousands of years.

This microwave radiation has a wavelength of ~1 millimeter to ~1 meter and is invisible to the human eye, only picked up by radio telescopes such as the VLA. The VLA measures these signals in terms of flux density, which is measured in Janskys where 1 Jy = 10^{-26} W / (m^2 * Hz) or energy over time over area per wavelength of the microwave radiation (e.g., Sojka et al., 2024). In addition, these light waves can be polarized, where all the photons in a given signal propagate through space similarly. Linearly polarized light has the electric field of the electromagnetic waves oscillating in the same planar direction, whilst circularly polarized light has the electric field vectors moving in the same cylindrical direction. This rotational direction is denoted by left and right hand polarization, or counter-clockwise and clockwise, respectively. The Stokes parameters IQUV indicate polarization, as I is the total signal intensity, Q/U are the linearly polarized signal intensities, and V is the circularly polarized signal intensity.

Among the different types of maser lines in the Orion Nebula, there are masers emitted by methanol molecules, i.e., methanol masers. Each maser type differs from other maser types.

For example, hydroxide masers typically have circular polarization whilst some formaldehyde masers have flares (Araya et al., 2010). Most previously discovered methanol masers in other regions have no polarization. In addition, instead of maser radiation, the same quantum transition could be detected in emission due to thermal excitation (e.g., Voronkov et al., 2005, Sanchez-Tovar et al., 2024). In this study, we look at the only previously discovered methanol maser in the region being studied by the VOLS collaboration.

Objectives

Our project had three main objectives pertaining to the characterization of this previously discovered methanol maser. The first objective was to confirm its initial flux density measurements using overlapping pointings. This maser appeared in the overlap between pointings from the VLA telescope, so we had two separate measurements of flux density for each epoch. We compared these measurements to check if signal strength was consistent or if it varied, indicating a telescope error or the presence of something affecting the maser.

The second objective was to check for fast variability, or when a maser changes its flux density in a very short time frame. The VLA telescope does two scans of each pointing within 60-80 min of each other during each epoch. If the flux density varies between the scans, this could indicate fast variability where the maser changes signal strength very quickly.

The third objective was to check for linear polarization. Using Stokes parameters on our data, we can extract information about the polarization of different light waves the VLA

telescope received. If we see a large prominence in linear or circular polarization, that can tell us more about how the maser is being excited and what type of stellar object it came from.

Methods

We used the virtual machines of the Jetstream2 service hosted in the computer supercluster at the University of Indiana and offered by the NSF (National Science Foundation) ACCESS program. We used a 32-core instance with Jetstream2 and the CASA program (Common Astronomy Software Applications) to conduct data analysis and spectral imaging.

We used multiple applications from CASA including **`tclean`**, **`listobs`**, **`plotms`**, **`imsubimage`**, and **`immath`** in order to organize our data and extract information from them. We used **`listobs`** for initialization and path management and **`immath/imsubimage`** for running calculations and extracting data. We used **`tclean`** to generate images from our interferometric data and remove the point-spread function from our images and **`plotms`** to graph different data axes we had.

When light hits the antennae of the VLA telescope, the light spreads out, causing the image to show streaks around the main signal point. The function that goes from the initial point where the light hits to the image of the streaks is called the point-spread function, also known as the synthesized beam (technically speaking, the effect of the point-spread function is convolved with the data, and is seen after the inverse Fourier transform of the amplitude and phases from the interferometer). The task **`tclean`** takes an image convolved with the synthesized beam and

removes some of the signal and associated point-spread function over and over in order to remove the effect of the point-spread function on the image. We also used a 2D Gaussian fit on the detections to generate a mathematical model for the distribution of the signal in the sky.

Spectral imaging was used to locate the channels where the signal was present and to graph the flux density over radio velocity. This allowed us to examine the maser's velocity relative to the Local Standard of Rest (a reference frame centered at the location of the Solar System, traveling around the Galaxy in a circular orbit). Many other graphs including characterizations of signal, characterizations of noise, and 1D Gaussian fits of the spectra were created and analyzed in order to better describe the maser.

Results & Discussion

For objective 1, we compared the flux density reading of each pointing to check if the maser's flux density was consistent on a short timescale. Epochs 1, 3, 5-17, and 19-20 were consistent, while epochs 2, 4, and 18 were inconsistent. Overall, we had 17 consistent epochs and 3 inconsistent epochs in our data set, with measurement values for flux density shown in Figure 1. The data points are separated by epoch in a grid structure. Each flux density reading had a signal point and a 3-sigma error bar. If the error bars for each pointing were not touching, then the pointings were inconsistent, and if they were, then the pointings were consistent. The red data points refer to pointing 73 (P73) and the blue data points refer to pointing 53 (P53).

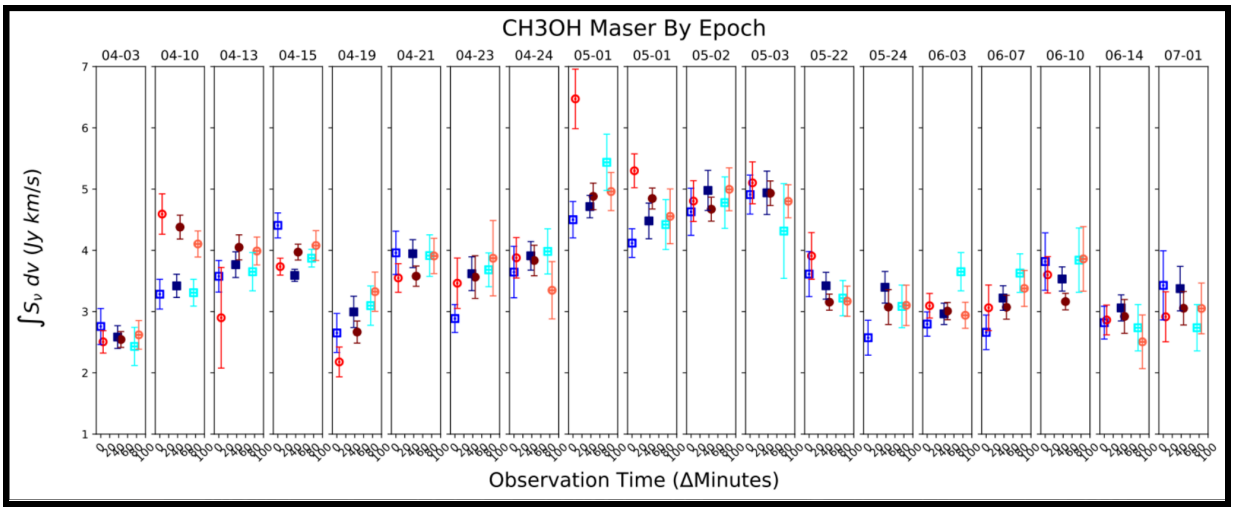

Figure 1: A graph of the flux density readings for the scans and pointing averages of each epoch [hollow red circles are scans of P73, hollow blue squares are scans of P53, filled-in dark red circles are P73 scan averages, and filled-in dark blue squares are P53 scan averages].

For objective 2, we created a light curve for each epoch to look at the flux density reading for each scan that the pointings are averaged from. Each pointing average corresponds to two scans. If you could draw a line through all of the error bars on the light curve, one could say that epoch is consistent. If one or more signals deviate significantly away from the others, then that epoch is inconsistent. Fast variability on a short time scale could be present if an epoch is inconsistent or had a general trend (a clear upwards or downwards change over time). An example of this process is in Figure 4.

In Figure 2, we used arrows to signal which epochs had low evidence of fast variability due to general consistency over time and which epochs had more evidence of fast variability. While these trends don't have enough evidence to say for sure that this maser presents fast variability in a consistent pattern, multiple interesting features of certain epochs point to places

where further research into the maser should be done. In epochs 9-12 (May 1st to May 3rd), we see a clear flare (cluster of higher flux density readings) along with more epochs with fast variability evidence. Nearby epochs are generally consistent, signalling that the flare was possibly caused by some external energy source.

When an external energy source hits the maser, the maser's molecules jump to a higher energy state before moving back down once hit by stray photons in a similar process to when the maser was first formed. Jumps in energy form flares that end once most of the maser's molecules jump down to a lower energy state. Possible causes include a nearby young stellar object, that the maser may have originated from, having its accretion disk grow, leading to a bigger radiation field or a shockwave front from another stellar object's evolution. Both of these events can lead to the input of energy into the maser if they happen close enough to the maser.

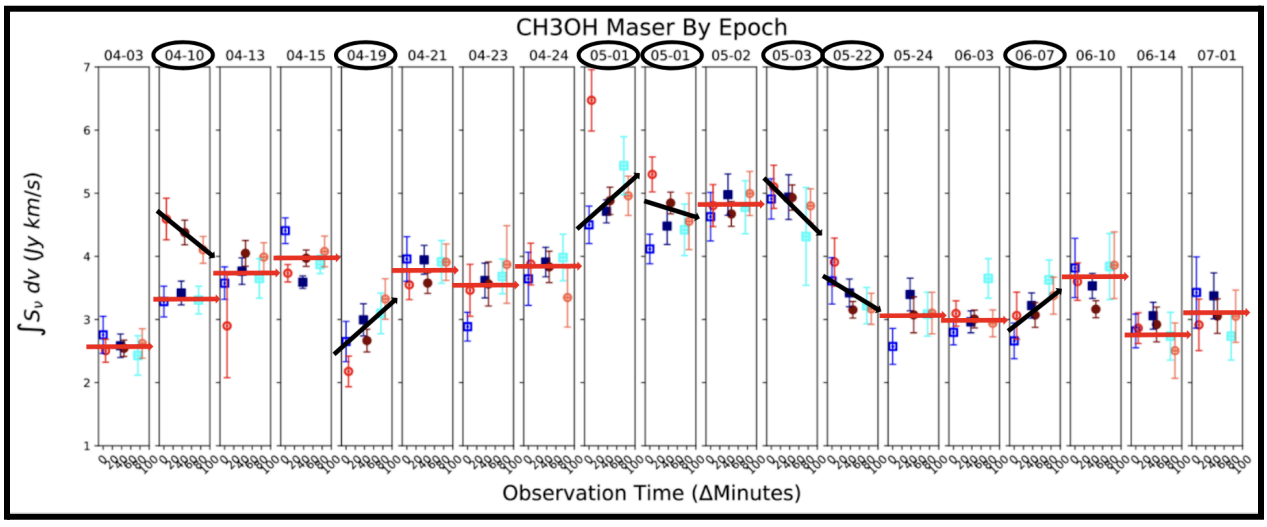

Figure 2: The same graph as in Figure 1, but with red arrows outlining epochs with low fast variability and black arrows outlining epochs with high fast variability, with the high fast variability epochs circled for emphasis. Same key is used.

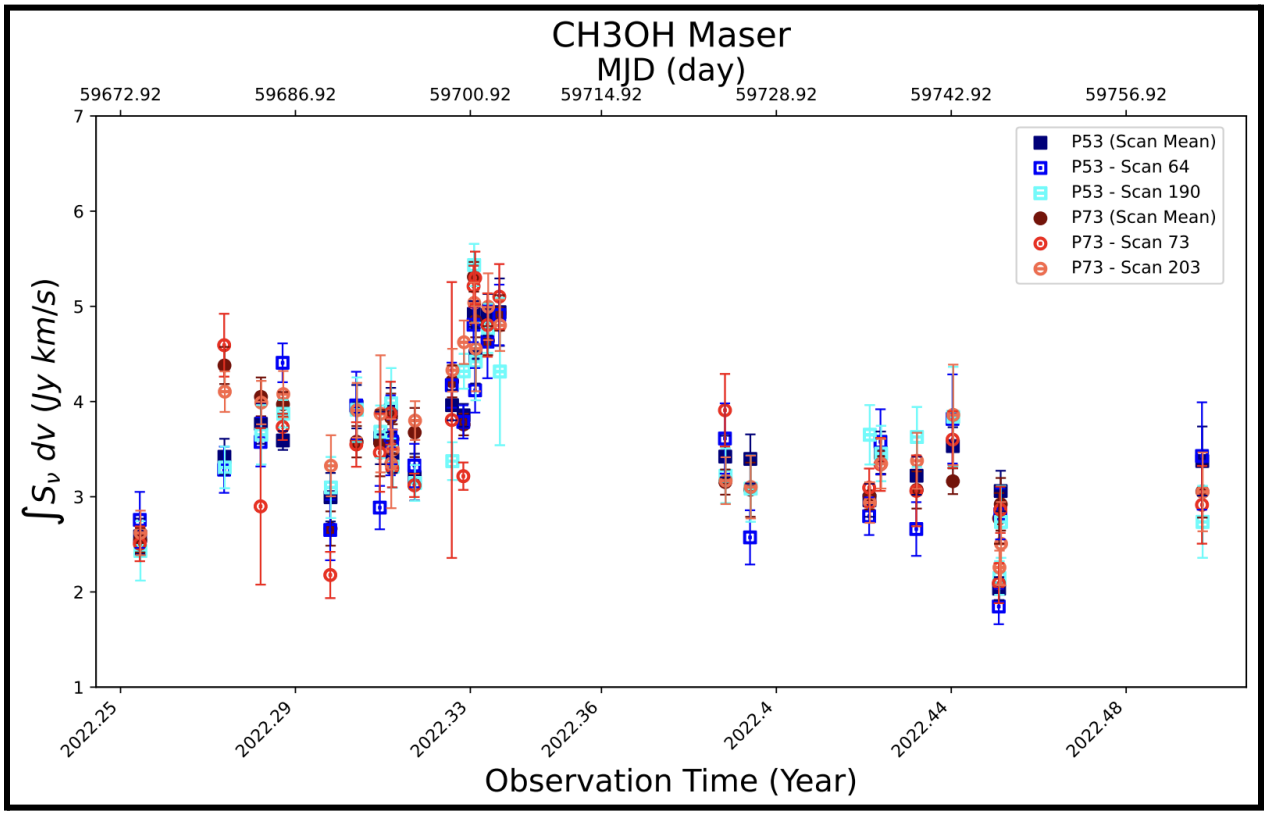

Figure 3: A graph of each flux density reading for the scans and pointing averages but on a consistent time-scale instead of epoch-by-epoch like in Figure 1 and Figure 2. Same key is used.

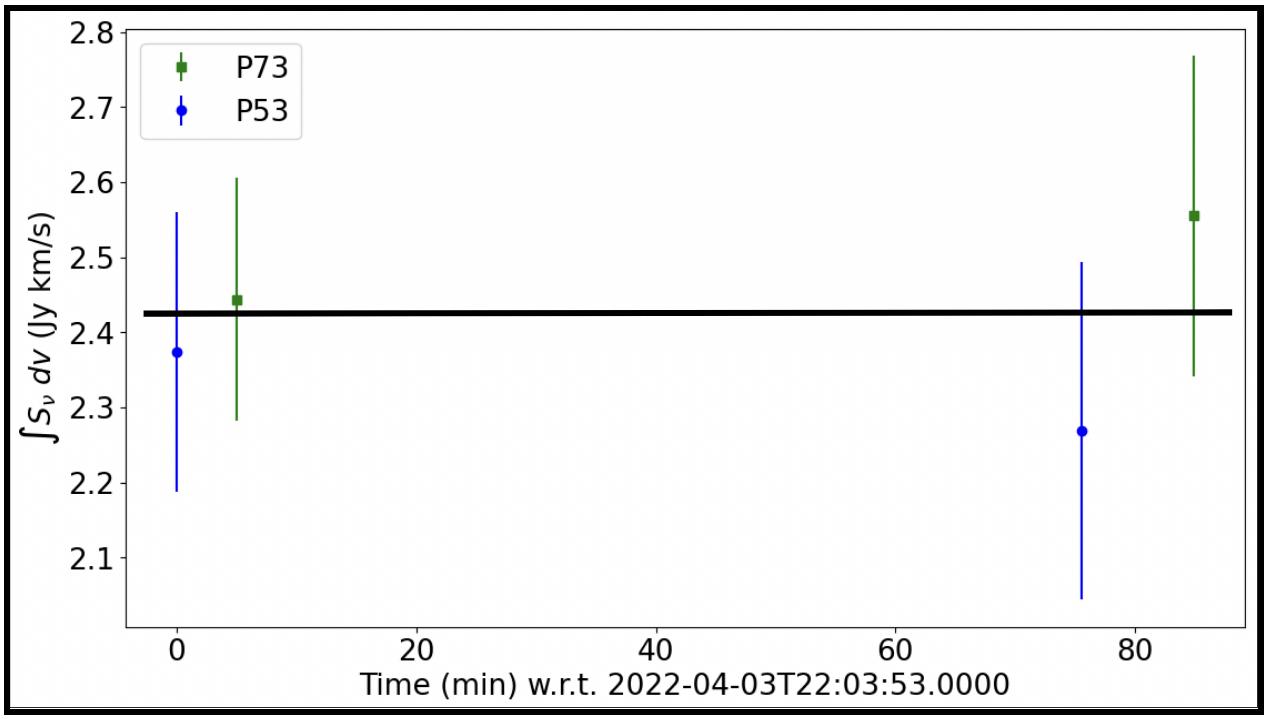

Figure 4: A light curve of all four scans in epoch 1, along with a horizontal line through all of them showing consistency between all four scans [P53 refers to measurements from pointing 53 and P73 refers to measurements from pointing 73].

For objective 3, we found no evidence of light wave polarization for any of the 20 epochs, which is consistent with previous literature's findings on the polarization of methanol masers. We looked at the IQUV Stokes parameters for linear and circular polarization, in which we found no net polarization and no dominant polarization angle for each epoch.

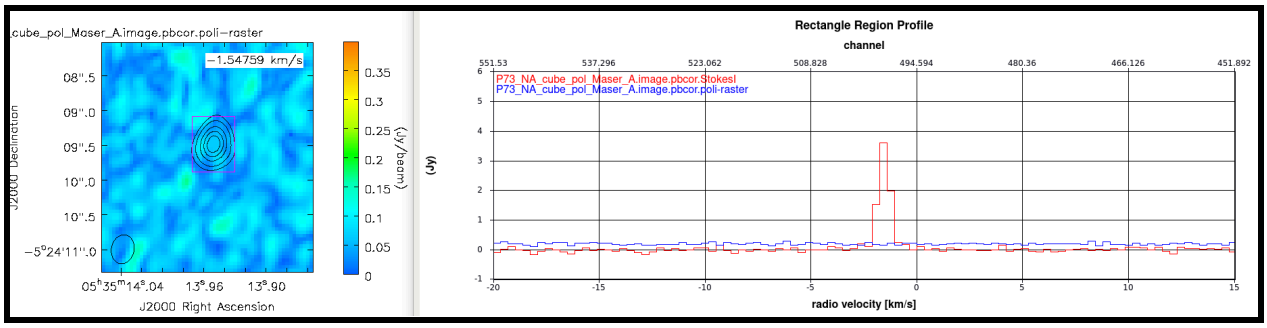

Figure 5: An image of the average polarization signal of all three polarization parameters QUV in epoch 1, along with a spectral line graph of the channel [black line contours show where the signal is, and the red graph shows the signal intensity while the blue graph shows the polarization intensity].

We also ran into a variety of epoch-specific discrepancies relating to different processes or unusual results in objectives 1 and 2. Below is a look at each discrepancy and how we found it in that epoch.

Figure 6 shows the light curve (flux density readings over time) of epoch 2, where we had particularly strange scan and pointing measurements. Each pointing is an average of two scans, with the flux density of each scan represented as a datapoint in Figure 6. Green data points are from pointing 73 and blue data points are from pointing 53. In both pointings, the averages of each scan pair are not between the individual readings for each scan, meaning the pointing averages are inconsistent in some way. Additionally, the flux density values of all four scans are distanced away from each other, showing inconsistency on a short timescale. The scans in each scan pair are consistent with each other, but the scan pairs themselves are inconsistent, suggesting a systematic offset of one pointing moving away from the other.

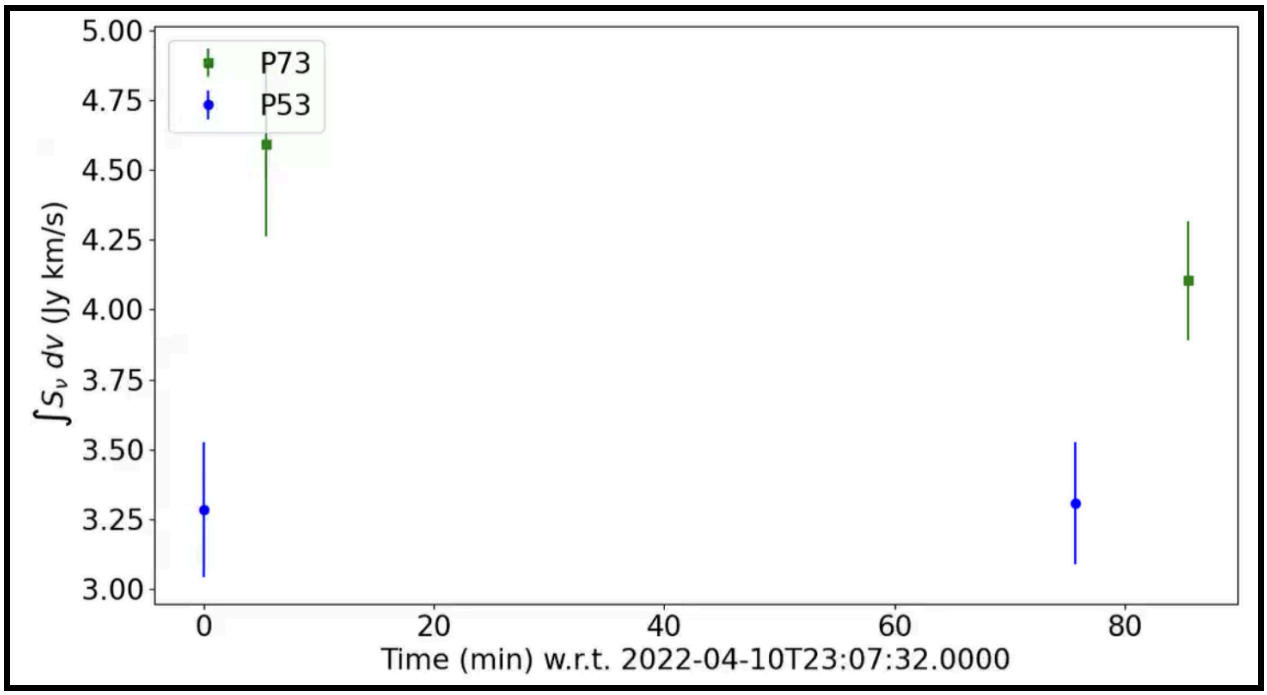

Figure 6: A light curve of all four scans in epoch 2.

Possible explanations for this behavior include telescope calibration errors and weather/ionosphere phenomena. A telescope error could offset the scans from each other, as the signal image is not captured correctly in some way. A weather/ionosphere phenomenon could cause parts of the signal to get delayed when light waves are traveling to the telescope, offsetting the interference pattern and changing the overall flux density of the scan. It's unlikely that this behavior is caused by astronomical phenomena as the behavior seems to be systematic.

As shown in Figure 8 (epoch 3), one of the scans (scan 73) is shifted down, while all the other scans are consistent with each other. Some of the telescopes malfunctioned and did not take data on scan 73, as shown by the missing baselines in Figure 8 (baselines are the distance between each pair of telescopes taking data, so less baselines means less telescope pairs were taking data). This in turn caused scan 73's spectral imaging to have more noise and less signal,

causing a lower signal-to-noise ratio. The image of the maser (displayed in Figure 9) shows an elongated source instead of a circular one due to some of the telescopes not taking data in one direction, causing signal uncertainty and smearing the signal along that direction.

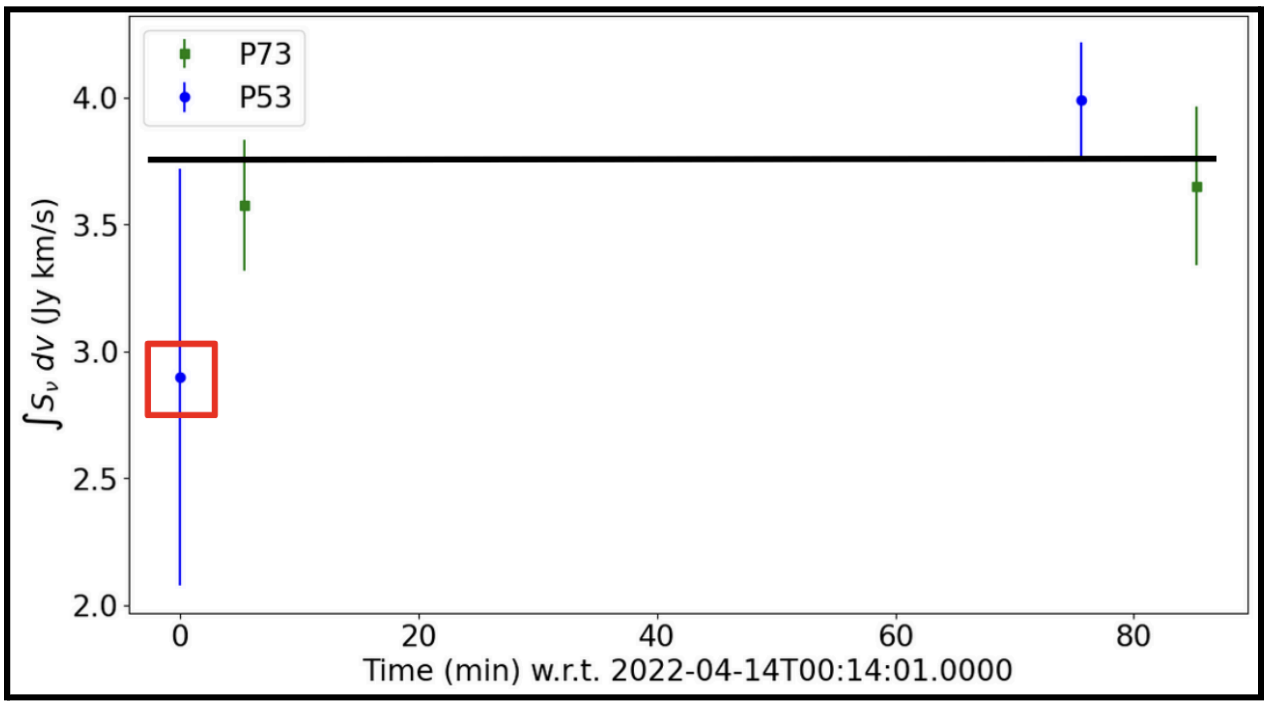

Figure 7: A light curve of all four scans in epoch 3, along with a horizontal line to show consistency between three of the scans and a red box to highlight scan 73's data point.

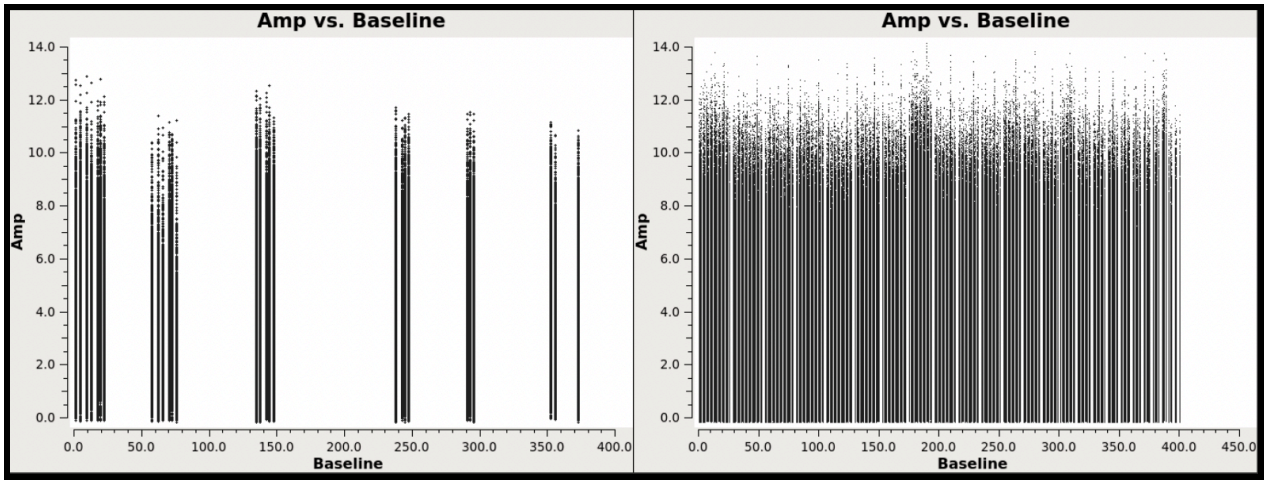

Figure 8: A graph of the telescope pairs for scan 73 (left) and scan 203 (right) in epoch 3.

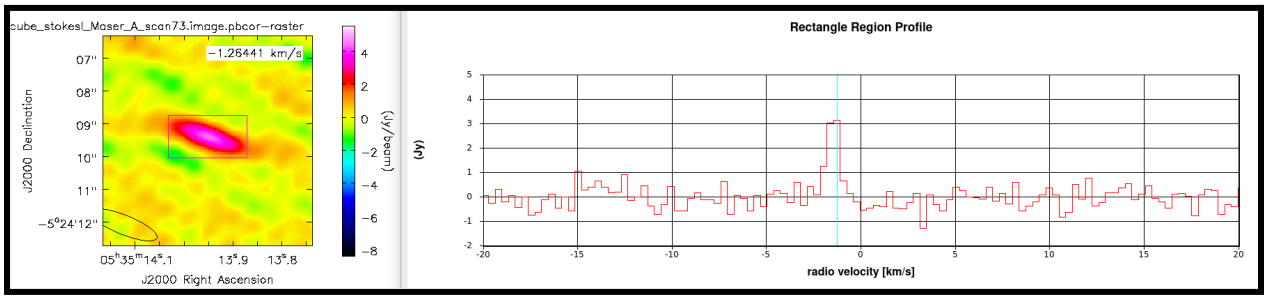

Figure 9: An image of scan 73, epoch 3 along with a spectral line graph of the channel.

Shown in Figure 10, epoch 10 (and mildly in some other epochs such as epochs 8 and 9) had negative sidelobes appear around the maser. We accounted for this occurrence by creating elliptical regions instead of rectangular regions. These negative sidelobes, if included in the region, would give a negative flux density reading for their pixels, decreasing the overall flux density value calculated from the region. Usually, if the region captures a small amount of positive and negative noise around the signal, not much of an offset is applied to the flux density value as the average of the noise is close to 0. However, negative sidelobes that are more severe in certain scans can create noticeable offset.

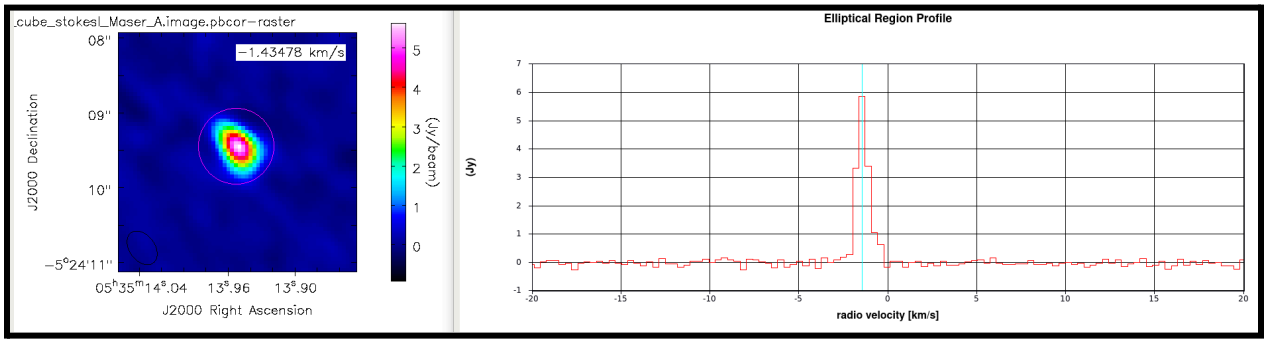

Figure 10: A signal image of pointing 73, epoch 10, where an elliptical region was used to prevent the capture of negative sidelobes (dark spots near the edge of the region).

Figure 11 shows an error log in epoch 11 (and oddly not in other epochs), where we ran into a repeated **`tclean`** masking error. The message log implies that **`tclean`** tried to run a process amidst another process's runtime, causing the program to error after only applying a few iterations. For many scans, no matter how high our **`n-iter`** variable was (number of iterations), only 9 iterations would be run per **`tclean`** process, in contrast to the 2000-2500 iterations needed for a complete image convolution for most scans in this study. This error can be overcome to some extent by cancelling the **`tclean`** after the error appears and running it again with the "go" command without changing the input. The error also appears to be related to **`tclean`**'s GUI (Graphical User Interface) as when the **`interactive`** variable is set to false to disable the GUI, **`tclean`** runs faster, though the error still appears.

```
0%....10....20....30....40....50....60....70....80....90....100%
2024-12-11 05:21:51     WARN    task_tclean::SIImageStore::getPSFGaussian (file src/code/synthesis/ImagerObjects/SIImageS
tore.cc, line 2038)     PSF is blank for[C0:P0] [C1:P0] [C2:P0] [C3:P0] [C4:P0] [C5:P0] [C6:P0] [C7:P0] [C8:P0] [C9:P0] [
C10:P0] [C1012:P0] [C1013:P0] [C1014:P0] [C1015:P0] [C1016:P0] [C1017:P0] [C1018:P0] [C1019:P0] [C1020:P0] [C1021:P0] [C1
022:P0] [C1023:P0]

0%....10....20....30....40....50....60....70....80....90....100%

0%....10....20....30....40....50....60....70....80....90....100%
2024-12-11 05:43:40     WARN    task_tclean::SynthesisImagerVi2::runCubeGridding (file src/code/synthesis/ImagerObjects/S
ynthesisImagerVi2.cc, line 1572)        Error : Error in copying internal T/F mask : Error in deleting internal T/F mask
: Region mask0 could not be removed
2024-12-11 05:43:40     WARN    task_tclean::SynthesisImagerVi2::runCubeGridding (file src/code/synthesis/ImagerObjects/S
ynthesisImagerVi2.cc, line 1572)+       Cannot delete the mask (used in another process)
```

Figure 11: The terminal output log of a ***tclean*** *process running into a mask error.*

Interestingly, this error occurred on all of the pointings and scans, but only stopped **tclean** from running fully for pointing 53, scan 73, and scan 190. **tclean** would show noticeable beam deconvolution progress on the image for around 2000 iterations before failing, but the error message would always appear even if **tclean** worked normally. We used the workaround described above for these scans, but the signal-to-noise ratio was noticeably lower and the RMS (root mean squared, a measure of noise in a dataset) was noticeably higher, meaning more noise was present around the signal in these images.

Summary

Our study covered three main objectives, aiming to characterize a methanol maser in the Orion Nebula. For objective 1, every epoch was consistent except for epochs 2, 4, and 18. For objective 2, no conclusive evidence of fast variability was found for the maser, although the data points showed interesting trends in some epochs that signified fast variability. For objective 3, we found no dominant polarization in any of the epochs. We had some epoch-specific discrepancies, with some explained/solved and some unexplained. For epoch 2, we saw

discrepancies with the pointing averages being offset and far away from each other. For epoch 3, we had an offset scan due to a lack of telescope data. For epoch 10 (and some others), we saw negative sidelobe features on our signal imaging, causing us to use elliptical regions for some scans/pointings instead of rectangular regions. For epoch 11, a tClean masking error occurred which made the process of tClean significantly slower. However, most of the spectral images were not affected, except for some extra noise on some of the scans. Through the analysis of the VLA data, we were able to characterize the maser on a series of short time-scales in this study. However, more epochs of data and new calibrations of previous datasets could help us further our study of this maser during future research.

References

Araya, E. D., Hofner, P., Goss, W. M., Kurtz, S., Richards, S., Linz, H., L. Olmi, & M. Sewiło. (2010). Quasi-periodic Formaldehyde Maser Flares in the Massive Protostellar Object IRAS 18566+0408. *The Astrophysical Journal Letters*, *717*(2), L133–L137. https://doi.org/10.1088/2041-8205/717/2/l133

Motte, F., Bontemps, S., & Louvet, F. (2018). High-Mass Star and Massive Cluster Formation in the Milky Way. *Annual Review of Astronomy and Astrophysics*, *56*(1), 41–82. https://doi.org/10.1146/annurev-astro-091916-055235

Sanchez-Tovar, E., Araya, E. D., Rosero, V., Hofner, P., & Kurtz, S. (2023). Broadband VLA Spectral-line Survey of a Sample of Ionized Jet Candidates. *The Astrophysical Journal Supplement Series*, *267*(2), 43. https://doi.org/10.3847/1538-4365/acdb5e

Sojka, G., VanZuiden, K., Araya, E., Busquet, G., Girart, J. M., Hofner, P., Fernández-López, M., Teixeira, P., Sánchez-Monge, A., Carrasco-González, C., Tobin, J., Rodríguez, T., &

VOLS. (2024). Changes in the Spectral Zoo: Preliminary Results of Molecular Maser Variability in VOLS. *Bulletin of the AAS*, *56*(7). https://baas.aas.org/pub/2024n7i302p06/release/1

Voronkov, M. A., Sobolev, A. M., Ellingsen, S. P., & Ostrovskii, A. B. (2005). The 6.7- and 25-GHz methanol masers in OMC-1. *Monthly Notices of the Royal Astronomical Society*, *362*(3), 995–1005. https://doi.org/10.1111/j.1365-2966.2005.09374.x